


Distinct roles of programmed death ligand 1 alternative splicing isoforms in colorectal cancer

Chaoyan Wang¹  | Menghan Weng¹ | Shuli Xia¹ | Min Zhang¹ | Chaoyi Chen¹ | Jinlong Tang¹ | Dan Huang² | Hongfei Yu¹ | Wenjie Sun¹ | Honghe Zhang¹ | Maode Lai^{1,3}

¹Department of Pathology, Research Unit of Intelligence Classification of Tumor Pathology and Precision Therapy of Chinese Academy of Medical Sciences (2019RU042), Zhejiang University School of Medicine, Hangzhou, China

²Department of Pathology, Fudan University Shanghai Cancer Center, Shanghai, China

³Department of Pharmacology, China Pharmaceutical University, Nanjing, China

Correspondence

Honghe Zhang, Department of Pathology, Zhejiang University School of Medicine, Hangzhou, China.

Email: honghezhang@zju.edu.cn

Maode Lai, Department of Pathology, Zhejiang University School of Medicine, Hangzhou, China; Department of Pharmacology, China Pharmaceutical University, Nanjing, China. Email: lmp@zju.edu.cn

Funding information

the 111 Project, Grant/Award Number: B13026; the National Natural Science Foundation of China, Grant/Award Number: 81672730, 81871937, 82072629 and 91859204

Abstract

Although anti-programmed death-1 (PD-1)/programmed death ligand 1 (PD-L1) immunotherapy has achieved great success in some cancers, most colorectal cancer (CRC) patients remain unresponsive. Therefore, further clarification of the underlying mechanisms is needed to improve the therapy. In this study, we explored the distinct functions of different PD-L1 alternative splicing isoforms in CRC. We investigated the biological functions in PD-L1 knocked down/knockout cells, which were verified through overexpression of PD-L1 isoforms a, b, and c. The roles of PD-L1 isoforms in immune surveillance resistance was also analyzed. Meanwhile, we performed RNA-seq to screen the downstream molecules regulated by PD-L1 isoforms. Finally, we detected PD-L1 and PD-L1 isoforms levels in a cohort of serum samples, two cohorts of CRC tissue samples, and analyzed the correlation of PD-L1 isoforms with PD-1 blockade therapy response in two clinical CRC cases. The results indicated that PD-L1 knockout inhibited proliferation, migration, and invasion, and isoform b exerted a more significant inhibitory effect on T cells than the other two isoforms. Moreover, isoform c could promote CRC progression through regulating epithelial-mesenchymal transition. Clinical data showed that CRC patients with positive PD-L1 expression were associated with poorer overall survival. High serum PD-L1 level was associated with poor prognosis. The level of isoform b or c was negatively associated with prognosis, and a higher level of isoform b was associated with a good response to anti-PD-1 therapy. In conclusion, isoform b should be considered as a biomarker for clinical responsiveness to anti-PD-1/PD-L1 immunotherapy; isoform c had a pro-metastatic role and is a new potential target for CRC therapy.

KEYWORDS

alternative splicing, colorectal cancer, immunotherapy, isoform, PD-L1

This is an open access article under the terms of the Creative Commons Attribution-NonCommercial License, which permits use, distribution and reproduction in any medium, provided the original work is properly cited and is not used for commercial purposes.

© 2020 The Authors. *Cancer Science* published by John Wiley & Sons Australia, Ltd on behalf of Japanese Cancer Association

1 | INTRODUCTION

As an important immune checkpoint, the programmed death-1 ligand 1 (PD-L1) interaction with programmed death-1 (PD-1) induces T-cell apoptosis and facilitates the escape of immune surveillance by tumor cells.^{1,2} PD-L1 is a type I transmembrane protein encoded by the CD274 gene in human chromosome 9 with 290 aa, which consists of extracellular domains (IgV-like domain, IgC-like domain, and the signal sequence domain), transmembrane domains, and intracellular domains.³ Besides binding to PD-1, PD-L1 could also bind to CD80 and provide an inhibitory signal to induce T-cell tolerance.^{4,5} The abnormal expression of PD-L1 has been reported in a variety of malignant tumors: for example, in lung cancer, breast cancer, ovarian cancer, malignant melanoma, renal cell carcinoma, hepatocellular carcinoma, and head and neck squamous cell carcinoma. The PD-L1 level is also closely related to tumor immune tolerance, immune evasion, and prognosis of patients.^{6–11} The high expression of PD-L1 in tumors also causes tumor immune escape, which promotes tumor growth and metastasis.¹² Although anti-PD-1/PD-L1 immunotherapy has achieved great success in melanoma^{13,14} and non-small cell lung cancer,¹⁵ unfortunately, the effect of this therapeutic in colorectal cancer (CRC) is not ideal and is closely related to high-level microsatellite instability/mismatch repair deficiency.¹⁶ Current clinical outcomes suggest that anti-PD-1/PD-L1 immunotherapy has substantial limitations in CRC. Therefore, the mechanism of the PD-1/PD-L1 pathway in CRC needs to be studied further. PD-L1, the key molecule of the PD-1/PD-L1 pathway, is rarely studied in CRC, and its function, molecular mechanism, and clinical significance in CRC need to be further clarified. Here, we report that the different PD-L1 alternative splicing isoforms play novel distinct roles in the regulation of immune surveillance and progression in CRC.

2 | MATERIALS AND METHODS

2.1 | Cell lines

The human CRC cell lines LS174T, DLD1, SW480, SW620, HCT8, HCT116, HT29, and RKO were purchased from the ATCC. The RKO mutant cell line RKO-MUT was already available in our laboratory. All the cells were cultured in RPMI 1640 medium (Gibco) supplemented with 10% FBS (Gibco) in an incubator with a 5% CO₂ atmosphere at 37°C. Interferon- γ (IFN- γ ; Peprotech) was used to treat colorectal cancer cells for 48 hours at a concentration of 25 ng/mL.¹⁷

2.2 | Clinical materials

Data for two CRC patients who suffered postoperative metastasis reoccurrence and treatment with PD-1 blockade therapy were obtained from Fudan University Shanghai Cancer Center. Three cohorts of samples, including 153 serum samples, 268 paraffin-embedded sections, and 139 cDNA samples from CRC patients, were

obtained from the Sir Run Run Shaw Hospital, Zhejiang University. A total of 153 serum samples from healthy control subjects were obtained during routine health examinations in the mean time. All patients received no preoperative chemotherapy or radiotherapy. The research protocols (2018018) were approved by the Ethics Committee of Zhejiang University School of Medicine.

2.3 | Transfection of oligos and vectors

All oligos, siRNA, and primers are included in Table S2. The nonviral expression vectors pcDNA3.1-isoform a-flag, pcDNA3.1-isoform b-ha, and pcDNA3.1-isoform c-myc were constructed by GenScript. The lentiviral expression vectors pLent-isoform a-flag-his, pLent-isoform b-ha-his, and pLent-isoform c-myc-his were constructed and packaged by Vigene. All the vectors were confirmed by DNA sequencing. The transfection of siRNA and nonviral expression vectors were conducted using the PowerFect In Vitro siRNA Transfection Kit (SigmaGen, Cat# SL100569) and Lipofectamine 2000 (Invitrogen, Cat# 11668-019) separately, then the biological function assays were performed after 48 hours of transfection. Cells transfected with lentiviral expression vectors were selected by puromycin (4 μ g/mL) to achieve higher expression efficiency.

2.4 | Generation of knockout cell lines

The CRISPR-Cas9 system was applied to generate knockout cell lines. We transfected the pLentiCRISPR v2 vector (GenScript, Cat# S58112), which encodes the sgRNA, into cells. Single-cell clones were expanded after puromycin selection (3 μ g/mL, 3 days). Sequencing and western blotting were used to validate the gene disruptions. The sgRNA sequence was TCTTTATATTCATGACCTAC.

2.5 | Cell proliferation assay

For proliferation assays, 2 \times 10³ cells were seeded into 96-well plates with 100 μ L of RPMI 1640 supplemented with 10% FBS using Cell Counting Kit (CCK8, Boster, Cat# AR1160) according to the manufacturer's instructions and then detected by a microplate reader (Bio-TEK, ELx 800, Saxony). The absorbance at 450 nm was measured. Each measurement was performed in triplicate, and the experiments were repeated three times.

2.6 | Cell migration and invasion assays

To evaluate the migratory and invasive capacities of cells, 24-well Transwell chambers with 8- μ m pore polycarbonate filter inserts (Corning, Cat#3422) were used. Cells were seeded at a density of 1 \times 10⁵ cells/well for the migration assay and 1 \times 10⁵ cells/well for the invasion assay. The cells were suspended in 100 μ L of serum-free

RPMI 1640 medium and placed in the upper compartment chambers. For the invasion assay, diluted extracellular matrix gel (BD Biosciences) was used to precoat the inserts for 30 minutes. The lower chambers were filled with 600 μ L of 10% FBS-supplemented RPMI 1640 medium as a chemoattractant. At the end of the experiments, the cells on the upper surface of the filters were removed, and the migrated cells on the lower surface were fixed in 4% paraformaldehyde and stained with 0.1% crystal violet. The migrated cells were then digested in 33% acetic acid and quantified by measuring the absorbance at 570 nm with a 96-well plate read by a microplate reader (Bio-TEK, ELx 800, Saxony). Three independent experiments were performed.

2.7 | Generation of human peripheral T lymphocytes

T cells were isolated directly from human whole blood with a human T-cell enrichment cocktail (STEMCELL, Cat#15021) and Ficoll density gradient centrifugation (STEMCELL, Cat#07801). Next, the T cells were activated with anti-CD3/CD28 beads (Gibco, Cat#11131D) and expanded for approximately 5 days. The T cells were grown in advanced RPMI 1640 medium supplemented with 2 mmol/L L-glutamine, 10% FBS, and recombinant human interleukin-2 (IL-2; 30 U/mL, Gibco, Cat#PHC0026). CD8⁺ T cells were isolated directly from human whole blood with a human CD8⁺ T-cell Isolation Kit (Miltenyi, Cat#130-096-495) and Ficoll density gradient centrifugation (STEMCELL, Cat#07801).

2.8 | Tumor cell-T-cell binding assay (apoptosis and cytotoxicity assay)

On day 5 of T-cell activation, expanded T cells were harvested and prepared for cocultivation. T-cell proliferation and apoptosis were then evaluated after coculture with control tumor cells or PD-L1 isoform-overexpressing tumor cells.

For the apoptosis assay, 1×10^5 tumor cells were cocultured with 5×10^5 T cells for 48 hours. Then, the nonadherent cells were collected in the supernatant of the cocultured cells, T cells were isolated from these mixed cells by flow cytometry by using staining with an anti-CD3 monoclonal antibody (Invitrogen, Cat#11-0036-42), and T cells were detected by flow cytometry by using an Annexin V-PE/7-AAD apoptosis kit (MultiSciences, Cat# AP104). Furthermore, 1×10^5 tumor cells were cocultured with 2.5×10^5 CD8⁺ T cells for 48 hours. Then, the nonadherent cells were collected in the supernatant, CD8⁺ T cells were isolated from these mixed cells by flow cytometry using staining with an anti-CD8 monoclonal antibody (Invitrogen, Cat#17-0088-42), and the Annexin FITC/PI apoptosis kit (MultiSciences, Cat# AP101) was used for flow cytometry assay.

For the cytotoxicity assay, 1×10^4 tumor cells were cocultured with 5×10^4 CD8⁺ T cells for 48 hours in a 96-well plate.

Specific lactate dehydrogenase (LDH) released from target cells in cell-free supernatant was detected using a cytotoxicity LDH detection kit (Genmed, Cat# GMS10073.1), following the manufacturer's instructions. The amount of LDH released was used to assess the lysis of target cells, which can be translated into the effectiveness of effector cells. The percent of cytotoxicity was calculated according to optical density (OD) values using the following formula: Cytotoxicity % = (Experimental - Effector spontaneous - Target spontaneous)/(Target maximum - Target spontaneous) \times 100%.

2.9 | ELISA

The concentrations of PD-L1 in the serum were detected using an ELISA kit (R&D Systems, Cat# DY156) according to the manufacturer's instructions.

A total of 2×10^5 PD-L1 isoform-overexpressing tumor cells or control tumor cells were cocultured with 1×10^6 T cells for 72 hours. ELISA kits (Multi Sciences, Cat# 70-EK1022, Cat# 70-EK180HS, and Cat# 70-EK1822) for detecting IL-2, IFN- γ , and tumor necrosis factor- α (TNF- α) were used to analyze the supernatants of the cocultured cells according to the manufacturer's instructions.

A total of 2×10^5 PD-L1 isoform-overexpressing tumor cells or control cells were cocultured with 5×10^5 CD8⁺ T cells for 72 hours. ELISA kits (MultiSciences, Cat# EK102, Cat# EK180HS, and Cat# EK182) for detecting IL-2, IFN- γ , and TNF- α were used to analyze the supernatants of the cocultured cells according to the manufacturer's instructions.

2.10 | RNA-Seq and Gene Ontology functional analysis

RNA was extracted from HCT116 EV cells (HCT116 cells transfected with the empty vector) and HCT116 cells overexpressing isoform a, b, or c, sequenced, and analyzed by RiboBio. All cells had three biological replicates. cDNA libraries were prepared from high-quality RNA using an Illumina TruSeq RNA sample prep kit following the manufacturer's instructions. Paired-end libraries were sequenced on an Illumina HiSeq 3000 sequencer (2 \times 150-bp read length). Clean reads were mapped to GRCh37 using STAR. Gene differential expression analysis was accomplished with Cuffdiff in the Cufflinks package, and the genes with $q < 0.05$ and $|\log_2(\text{fold change})| > 0.8$ were defined as differentially expressed genes (DEG) and were candidates for further analysis and quantitative PCR validation.

Gene expression heat map generation and hierarchical clustering were performed using Heatmapper (<http://www.heatmapper.ca/>). The Pearson correlation was selected as the distance metric; average linkage clustering was selected as the linkage method. Gene Ontology (GO) enrichment analysis was performed using DAVID

online tools (<http://david.abcc.ncifcrf.gov>). The results were visualized using the R package ggplot2 in R software.

2.11 | Quantitative PCR

We isolated RNA from cells and crushed tumor tissue samples using the TRIZOL method. cDNA was obtained using the PrimeScript RT Reagent Kit with gDNA Eraser (TaKaRa, Cat# RR047A) according to the manufacturer's instructions. SYBR Premix Ex Taq (TaKaRa, Cat# RR420A) was used to analyze gene expression by RT-PCR carried out using the ABI 7900 platform (Applied Biosystems). Relative mRNA levels were normalized to β -actin mRNA levels. The primers used are included in Table S2.

2.12 | Western blot analysis

Whole-cell lysates, cell culture medium which were ultra-filtrated and concentrated, were separated using 8%-10% SDS-PAGE and transferred onto nitrocellulose membranes (Bio-Rad, Laboratories). Then, the blots were blocked with 5% low-fat milk at room temperature for 1 hour and incubated overnight at 4°C with primary antibodies, followed by incubation with secondary antibodies (Odyssey, Li-COR, Bioscience) for 1 hour at room temperature. Finally, the membranes were developed with an Odyssey system. β -actin was used as a loading control. Information about the primary antibodies is provided in Table S1.

2.13 | Coimmunoprecipitation

HA-tagged PD-1, flag-tagged PD-L1 isoforms, and other indicated plasmids were cotransfected into HEK293 cells. The cells were lysed in RIPA lysis buffer (strong) after 48 hours of transfection and incubated with anti-flag magnetic beads overnight at 4°C. The immunoprecipitates were separated by SDS-PAGE and analyzed by western blotting. The process of the reverse immunoprecipitation assay was similar to that described above.

2.14 | Immunofluorescence staining

Established cell lines were seeded on slides. After the cells attached, they were fixed in 4% paraformaldehyde for 15 minutes at room temperature, washed three times with PBS, permeabilized with ice-cold 0.5% Triton X-100 for 20 minutes at room temperature, and then washed three times with PBS. The slides were blocked in PBS containing 10% FBS for 30 minutes at room temperature and then incubated with antibodies against PD-L1 overnight at 4°C, followed by incubation with fluorophore-conjugated secondary antibodies for 1 hour. Nuclei were stained with DAPI. Images were captured with a confocal microscope

(Olympus FV3000 OSR, Olympus). Assays were performed in triplicate.

2.15 | Immunohistochemistry

Paraffin-embedded sections were heated at 70°C for 30 minutes. Deparaffinization and rehydration were carried out in xylene and ethanol. After 3 minutes of high pressure-induced antigen retrieval, the sections were cooled to room temperature and sealed with 10% bovine serum for 15 minutes. Primary antibody (ZSGB-BIO, Cat# ZA-0629, 1:100 dilution) incubation was performed for 1.5 hours at 37°C. At room temperature, secondary antibody reinforcement fluid (ORIGENE, Cat# PV-9000) incubation was performed for 10 minutes, and secondary reactant working fluid (ORIGENE, Cat# PV-9000) incubation was performed for 30 minutes. Then, DAB color development and hematoxylin counterstaining were performed. The sections were then dehydrated in ethanol, cleared in xylene twice, and sealed with gum.

2.16 | In vivo mouse study

Four-week-old male NOD/SCID mice were obtained from Shanghai Laboratory Animal Center (SLAC). All animal handling procedures were approved by the Ethics Committee of Zhejiang University School of Medicine. An HCT116 CRC tumor model of splenic liver metastasis was established in the NOD/SCID mice. The mice were anesthetized by i.p. injection of 4% chloral hydrate (10 mg/mL) and placed in the supine position. We made a left abdominal incision to exteriorize the spleen and then injected 1×10^6 HCT116 cells to stably express luciferase into the edge of the spleen. We gently pressed on the injection site to avoid liquid leakage. The spleen was returned to the peritoneal cavity. The degree of metastasis and tumor burden were measured by i.p. injection of 100 μ L of D-luciferin (GOLDBIO, 150 mg/kg, 5 minutes prior to imaging), followed by bioluminescent analysis using an IVIS Spectrum imaging system (Caliper).

Male athymic nude mice (Balb/c nu/nu, 5 weeks old) were obtained from SLAC and housed under specific pathogen-free (SPF) conditions according to the guidelines of the Animal Care Committee. T cells were first transfected with pLenti-UTR-Luc-Blank Vector (abm, Cat# m012). Forty-eight hours after transfection, the T cells and PD-L1 isoform-overexpressing tumor cells or control tumor cells were mixed in PBS. For subcutaneous injections, 1×10^6 tumor cells and 5×10^6 T cells were resuspended in 100 μ L of PBS and injected into each mouse in the right inguinal region. The mice were monitored every day for T-cell survival by bioluminescence imaging until the bioluminescence signal was undetectable. The mice were injected with luciferin (150 mg/kg, 5 minutes prior to imaging), anesthetized with 3% isoflurane, and then imaged with an IVIS Spectrum imaging system (Caliper). Images were analyzed with Living Image

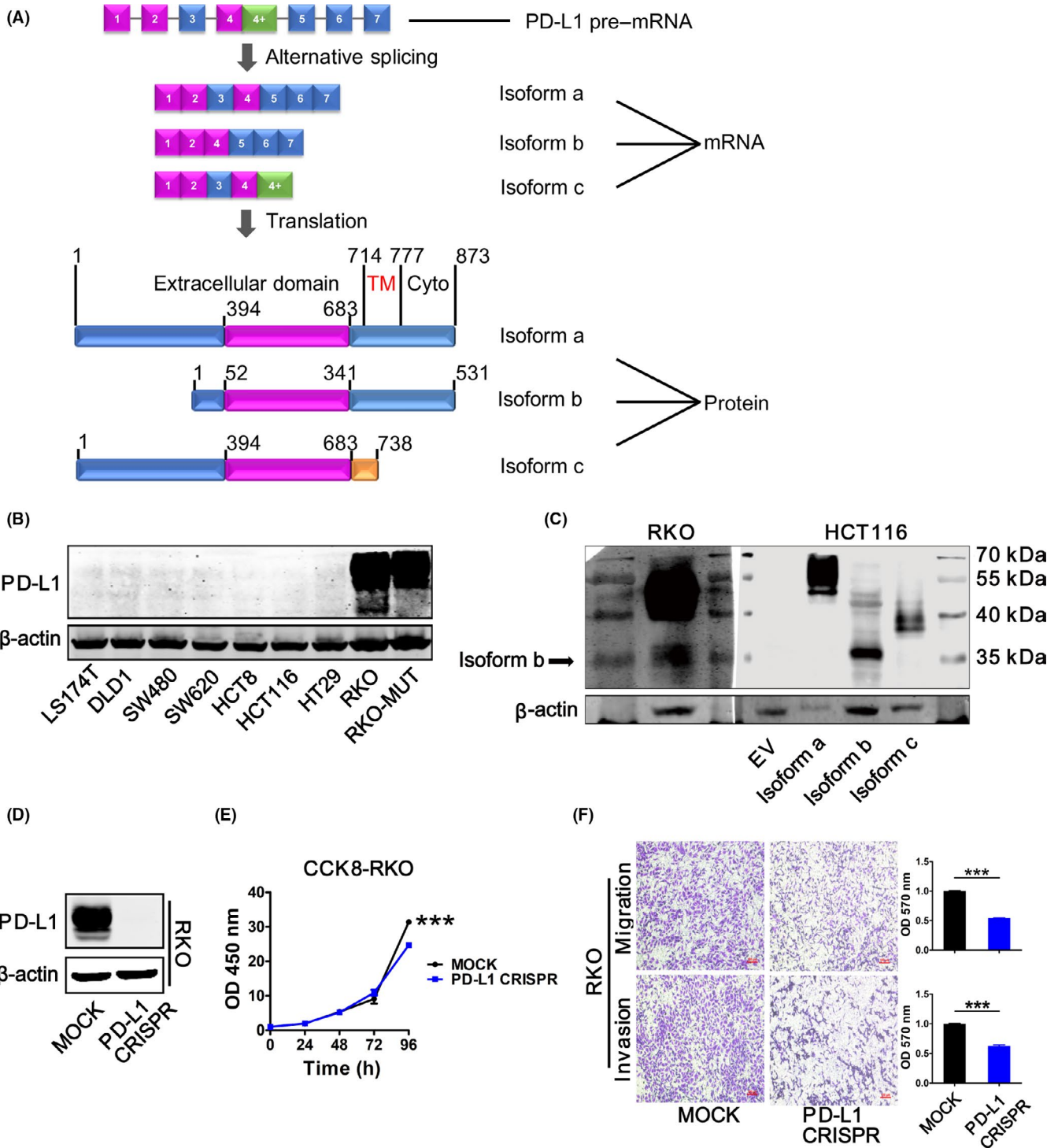


FIGURE 1 The expression and roles of PD-L1 in CRC cell lines. A, Schematic diagram of the structures of PD-L1 isoforms. B, Immunoblotting analysis of PD-L1 protein levels in CRC cell lines. C, Immunoblotting analysis of the PD-L1 protein levels in RKO cells and the PD-L1 isoform protein levels in HCT116 cells which overexpress the PD-L1 isoforms. D, Immunoblotting for the detection of PD-L1 expression in RKO cells with the PD-L1 gene knocked out using CRISPR-Cas9 technology. E, Cell Counting Kit-8 assay investigating the proliferative potential of RKO cells with the PD-L1 gene knocked out (the histograms on the right are for the quantification analysis). F, Migration (upper panel) and invasion (lower panel) assays with RKO cells with the PD-L1 gene knocked out (the histograms on the right are for the quantification analysis). Data are representative of three independent experiments and (E, F) were analyzed using an unpaired *t* test. Data are presented as mean \pm SD; **P* < 0.05, ***P* < 0.01, and ****P* < 0.001. CRC, colorectal cancer; OD, optical density; PD-L1, programmed death ligand 1; TM, transmembrane domain; Cyto, cytoplasmic domain

software (Caliper). Bioluminescent flux (photons/s/sr/cm²) was determined for the mixed-cell injection site.

2.17 | Statistical analysis

Each experiment was performed in triplicate and repeated at least three times. All statistical analyses were performed using GraphPad Prism v.6.0. (GraphPad, Software, San Diego, CA, USA) and SPSS 20.0. A two-tailed Student's *t* test was used to test for significant differences between two groups, and Welch's correction was applied when comparing groups with unequal variance (*F*-test $P < 0.05$). Overall survival was analyzed using the Kaplan-Meier method. The relationships among isoforms of PD-L1 mRNA level in CRC tissue samples was analyzed using the Kruskal-Wallis test. All data were presented as the mean \pm standard deviation or median. *P*-values < 0.05 were considered statistically significant (* $P < 0.05$, ** $P < 0.01$, and *** $P < 0.001$).

3 | RESULTS

3.1 | Programmed death ligand 1 expression in colorectal cancer cells and programmed death ligand 1 knockout inhibited colorectal cancer proliferation, migration, and invasion in vitro

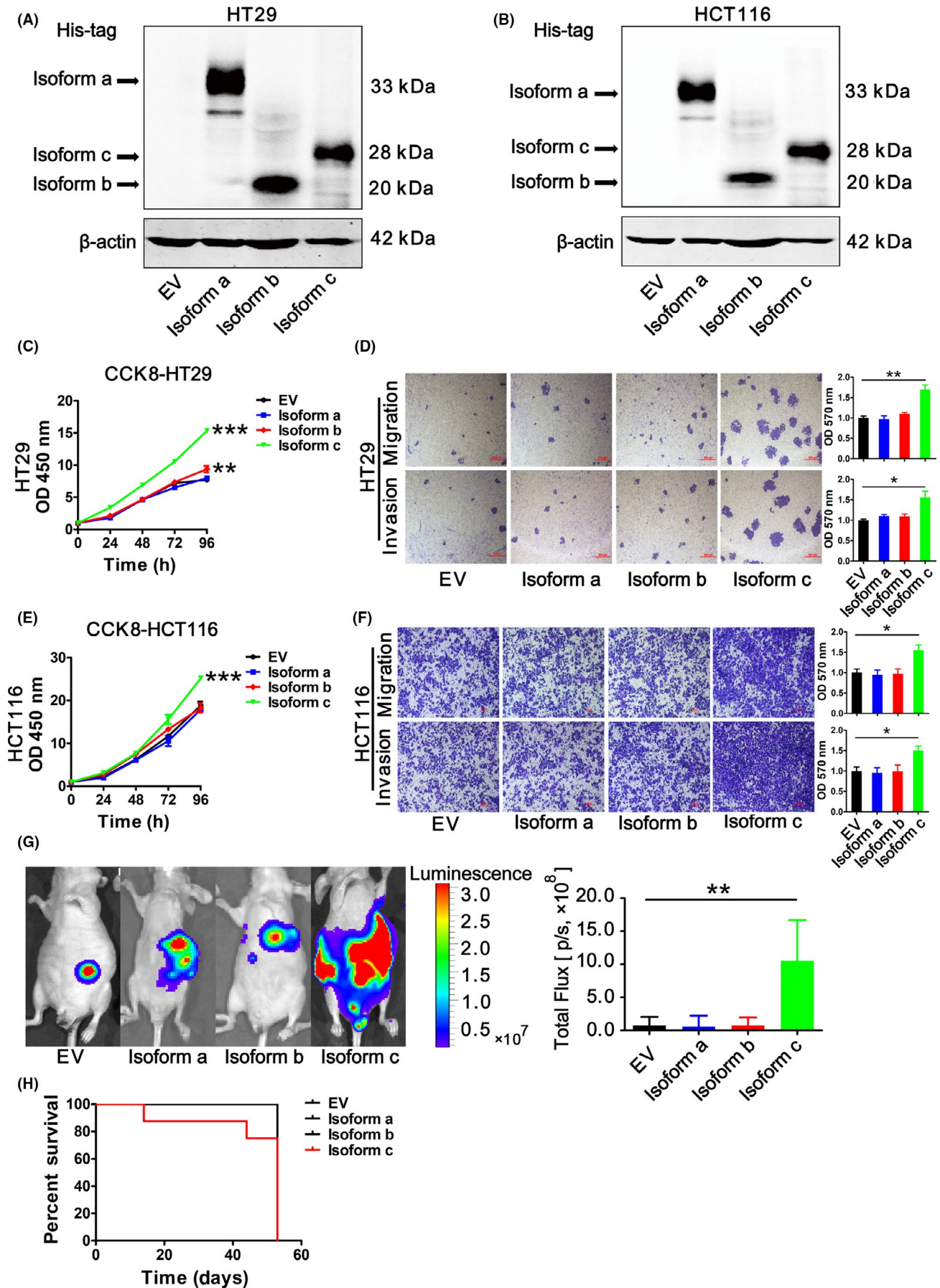
Alternative splicing is a key control point in gene expression that produces proteome diversity.^{18,19} In searching the US National Center for Biotechnology Information (NCBI) database, we found that PD-L1 pre-mRNA can generate three variants by alternative splicing, as shown in Figure 1A: isoform a, isoform b, and isoform c. Thus far, studies have considered isoform a to be the research target by default because it represents the full-length PD-L1 transcript. Compared with isoform a, isoform b lacks an exon in the 5' coding region, which leads to the production of a shorter protein than that produced from isoform a,²⁰ and isoform c carries a new 3' coding region and new 3'UTR, resulting in a protein with a different C-terminus. However, the biological roles of PD-L1 isoforms b and c remain unclear. First, we detected the expression of PD-L1 in CRC cell lines by immunoblotting, which showed that

RKO and RKO-variant cell lines have higher PD-L1 expression than other cell lines (Figure 1B). Interestingly, a nonspecific band was observed below the main band in RKO cells (Figure 1B). To validate whether the nonspecific band was a PD-L1 splicing isoform, we cloned the three isoforms into expression vectors and transected the vectors into HCT116 and HT29 cells. The results showed that PD-L1 isoforms a, b, and c could be overexpressed at both the mRNA and protein levels (Figure S1A,B). Interestingly, the molecular weight of the nonspecific band in RKO cells was consistent with PD-L1 isoform b, which might be considered the endogenous PD-L1 isoform b in CRC cells (Figure 1C). Then, knocking out PD-L1 in RKO cells (Figure 1D) using Crispr-Cas9 technology significantly inhibited proliferation (Figure 1E), migration, and invasion (Figure 1F). To avoid off-target effects, we knocked down PD-L1 expression using siRNA (Figure S1C), which showed a similar phenotype of decreased proliferation (Figure S1D), migration, and invasion (Figure S1E). Together with these results, we suggested that PD-L1 could promote proliferation, migration, and invasion of CRC.

3.2 | Programmed death ligand 1 isoform c role in promoting migration and invasion of colorectal cancer cells in vitro and in vivo

To test whether PD-L1 isoforms play biological roles in CRC, we stably overexpressed PD-L1 isoforms a, b, and c in HT29 (Figure 2A) and HCT116 cells (Figure 2B) and found that only the overexpression of PD-L1 isoform c promoted HT29 and HCT116 cell proliferation (Figure 2C,E), migration, and invasion (Figure 2D,F). When PD-L1 isoform c was overexpressed in PD-L1 knockout RKO cells (Figure S2A), the potential of proliferation, motility, and invasion were restored (Figure S2B,C). In vivo, more significant prometastatic signals were observed in mice expressing PD-L1 isoform c than in mice expressing the other isoforms (Figure 2G), and there was also poorer survival in mice orthotopically inoculated in the spleen with PD-L1 isoform c-expressing CRC cells than in mice orthotopically inoculated with CRC cells expressing the other isoforms (Figure 2H). Taken together, PD-L1 isoform c performed the role of PD-L1 in promoting proliferation, migration, and invasion in CRC.

FIGURE 2 The roles of different programmed death ligand 1 (PD-L1) isoforms in CRC cell proliferation, migration, and invasion in vitro and in vivo. A,B, Immunoblotting analysis of PD-L1 isoform protein levels in transfected HT29 (A) and HCT116 cells (B). These cells were transfected with the lentiviral expression vector pLent-EF1a-FH-CMV-Puro (EV), pLent-isoform a-flag-his, pLent-isoform b-ha-his, or pLent-isoform c-myc-his. C, Cell Counting Kit-8 (CCK-8) assay investigating the proliferative potential of HT29 cells overexpressing the PD-L1 isoforms. D, Migration (upper panel) and invasion (lower panel) assays with HT29 cells overexpressing the PD-L1 isoforms (the histograms on the right are for the quantification analysis). E, CCK-8 assay investigating the proliferative potential of HCT116 cells overexpressing the PD-L1 isoforms. F, Migration (upper panel) and invasion (lower panel) assays with HCT116 cells overexpressing the PD-L1 isoforms (the histograms on the right are for the quantification analysis). G, Representative bioluminescence images and statistical analysis for bioluminescence of the liver metastasis model established by splenic injection of HCT116-EV, HCT116-isoform a, HCT116-isoform b, and HCT116-isoform c cells. H, Kaplan-Meier plots for the overall survival of mice injected with HCT116 cells with PD-L1 isoform overexpression. Data are representative of three independent experiments and (C-F) were analyzed using an unpaired *t* test. Data are presented as mean \pm SD; * $P < 0.05$, ** $P < 0.01$, and *** $P < 0.001$. CRC, colorectal cancer; EV, empty vector; OD, optical density



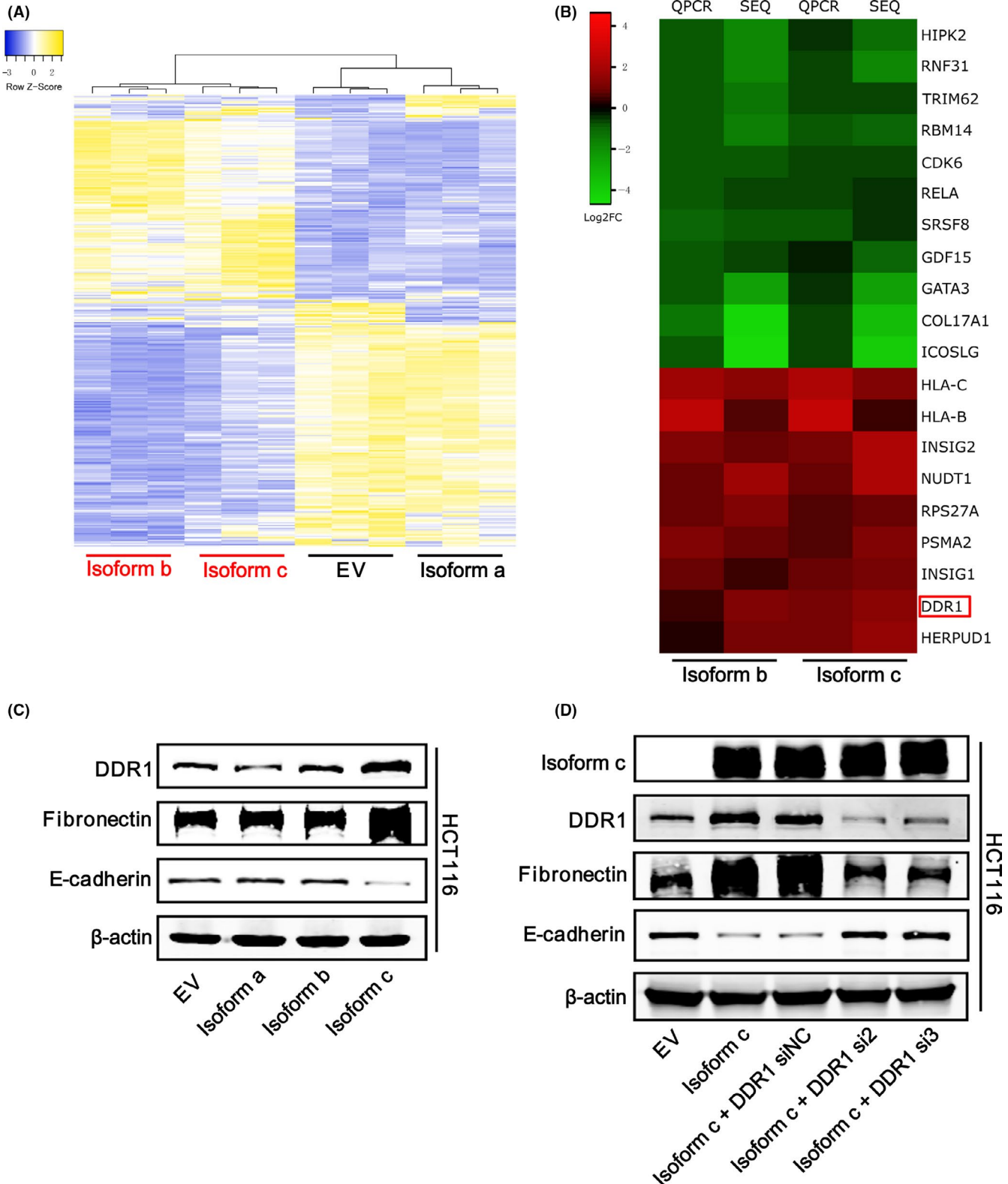


FIGURE 3 Programmed death ligand 1 (PD-L1) isoform c regulated colorectal cancer epithelial-mesenchymal transition via the upregulation of DDR1 expression. A, Heat map of the hierarchical clustering of the DEG regulated by PD-L1 isoforms a, b, and c in HCT116 cells. B, Heat map for the validation of the RNA-seq results of 20 DEG regulated by PD-L1 isoform b using quantitative RT-PCR. C, Immunoblotting analysis of the expression of DDR1, fibronectin, and E-cadherin in HCT116 cells overexpressing PD-L1 isoforms. D, Immunoblotting analysis of the expression of PD-L1 isoform c, DDR1, fibronectin, and E-cadherin in PD-L1 isoform c-overexpressing HCT116 cells and DDR1 expression knockdown HCT116 cells. Data are representative of three independent experiments. DEG, differentially expressed gene; EV, empty vector; FC, fold change; siDDR1, DDR1 expression knockdown; siNC, negative control siRNA

3.3 | Programmed death ligand 1 isoform c promoted colorectal cancer cell progression through regulating epithelial-mesenchymal transition

We next performed RNA-seq to investigate the downstream molecular signals of the PD-L1 isoforms in CRC. Hierarchical clustering revealed that the downstream gene expression patterns of PD-L1 isoforms b and c were more similar than those of either isoform a and the control (EV); however, compared with the control, PD-L1 isoform a did not regulate more DEG (Figure 3A). To validate the accuracy of the RNA-seq analysis, we individually measured 20 DEG regulated by PD-L1 isoforms b and c in HCT116 cells by quantitative RT-PCR (qRT-PCR), which showed expression changes consistent with those observed by RNA-seq (Figure 3B). Our previous results showed that PD-L1 isoform c could promote CRC metastasis; however, the mechanism remained unclear. Interestingly, among these DEG, discoidin domain receptor tyrosine kinase 1 (DDR1) showed significantly upregulated expression in response to PD-L1 isoform c, which has been demonstrated to function in a prometastatic role through inducing epithelial-mesenchymal transition (EMT).²¹ EMT plays an important role in the process of tumor metastasis and progression for CRC.²² As shown in Figure 3C, PD-L1 isoform c not only increased DDR1 expression but also enhanced fibronectin expression and inhibited E-cadherin expression. We used siRNA to knock down DDR1 expression in PD-L1 isoform c-overexpressing HCT116 cells. The results showed that DDR1 silencing rescued the expression of E-cadherin and reduced fibronectin expression (Figure 3D). Thus, PD-L1 isoform c is a prometastatic gene in CRC.

3.4 | Programmed death ligand 1 isoform b-mediated inhibitory effects on T cells in vitro and in vivo

We also investigated the biological functions of PD-L1 isoforms a, b, and c through GO (BP, biological process) enrichment analysis. Surprisingly, only the biological processes regulated by PD-L1 isoform b were enriched in the immune response, the drug response, T-cell activation, and T-cell receptor signaling pathways, while the other two isoforms were related to the inflammatory reaction, aging, transcriptional regulation, and the metabolic process (Figure S3A). To further research the immune surveillance resistance of PD-L1 isoforms, we cocultured T cells or CD8⁺ T cells and CRC cells with stable overexpression of isoform a, b, or c. Flow cytometry assays showed that CRC cells with overexpressing PD-L1 isoform b could significantly induce T cells apoptosis, but isoforms a and c did not affect T cell apoptosis significantly (Figure 4A). Overexpressing PD-L1 isoform b in CRC cells showed the most significant effect in inducing CD8⁺ T cells apoptosis (Figure 5A).

Cytotoxicity assays showed that CRC cells with PD-L1 isoform b overexpression could significantly decrease the cytotoxicity of

CD8⁺ T cells (Figure 5B). Because the secretion of the cytokines IL-2, IFN- γ , and TNF- α is usually considered a biomarker of T-cell activity,⁴ we detected the levels of IL-2, IFN- γ , and TNF- α in the supernatant of cocultures of T cells and PD-L1 isoform-overexpressing CRC cells. Compared with the control, PD-L1 isoform b significantly decreased the secretion of the cytokines IL-2, IFN- γ , and TNF- α by T cells, and PD-L1 isoform c decreased the secretion of IFN- γ and TNF- α by T cells (Figure 4B). More interestingly, PD-L1 isoform b significantly decreased the secretion of the cytokines IL-2, IFN- γ , and TNF- α by CD8⁺ T cells. PD-L1 isoform a and c decreased the secretion of IFN- γ and TNF- α by CD8⁺ T cells (Figure 5C). To test the effect of the PD-L1 isoforms on T cells in vivo, we subcutaneously injected luciferase-labeled T cells into nude mice together with isoform a, b, or c-overexpressing HCT116 cells and tested the mice through bioluminescent imaging to monitor the survival of the T cells. The results showed that the CRC cells overexpressing PD-L1 isoform b or c accelerated T-cell death and suppressed T-cell survival (Figure 4C). Collectively, we could conclude that PD-L1 isoform b showed the most significant inhibitory effect on T cells in vitro and vivo.

Because PD-L1 functions in immune suppressive roles by binding to PD-1,²³ we coexpressed Flag-labeled PD-L1 isoform a, b, or c in HEK293 cells together with HA-labeled PD-1. Interestingly, a coimmunoprecipitation (co-IP) assay with an anti-Flag antibody showed that only PD-L1 isoforms b and c could pull down PD-1 significantly; PD-L1 isoform a could only bind to PD-1 weakly (Figure 4D). Another co-IP assay with an anti-HA antibody revealed that PD-1 could also only significantly bind to PD-L1 isoforms b and c but not to isoform a (Figure 4E). Although PD-L1 isoform c could powerfully bind to PD-1, it had no significant suppressive effect on T cells. To address this point, we performed immunofluorescence assays to detect the subcellular localization of the PD-L1 isoforms, and these assays showed that PD-L1 isoforms a and b localized in the cytomembrane and cytoplasm, but isoform c localized only in the cytoplasm (Figure 5D and Figure S3C). In addition, to further verify the location of PD-L1 isoforms, we isolated cell nuclear, cytoplasmic, and membrane fractions, then detected each PD-L1 isoform protein by western blot, with similar results to immunofluorescence assays (Figure S3B). Together, these results suggested that PD-L1 isoform a exerted a weak immunological effect on T cells because the interaction with PD-1 was weak, even though PD-L1 isoform a was located in the cytomembrane. However, even though PD-L1 isoform c could bind to PD-1 well, because it was located in the cytoplasm, it did not participate in immunosuppression well. Only PD-L1 isoform b could interact with PD-1 strongly and localize to the cytomembrane, where it could negatively regulate T cells effectively.

As is well-known, PD-L1 is induced or maintained by many cytokines, such as interferon- γ (IFN- γ), tumor necrosis factor- α (TNF- α), vascular endothelial growth factor (VEGF), and granulocyte-macrophage colony-stimulating factor (GM-CSF) and so on, of which IFN- γ is the most important.^{9,24-26} However, in our study, IFN- γ treatment did not change the localization and amount of each

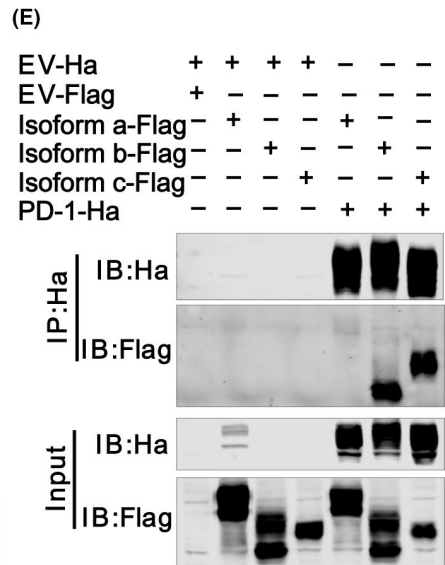
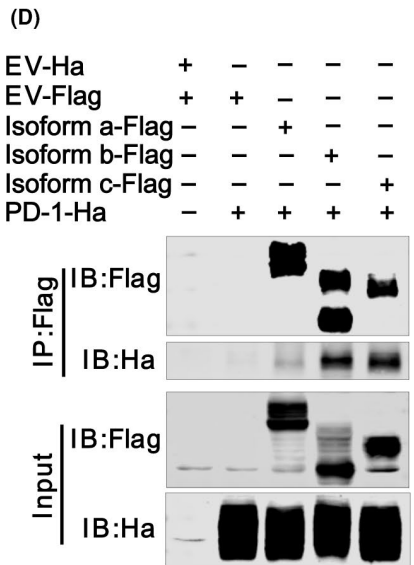
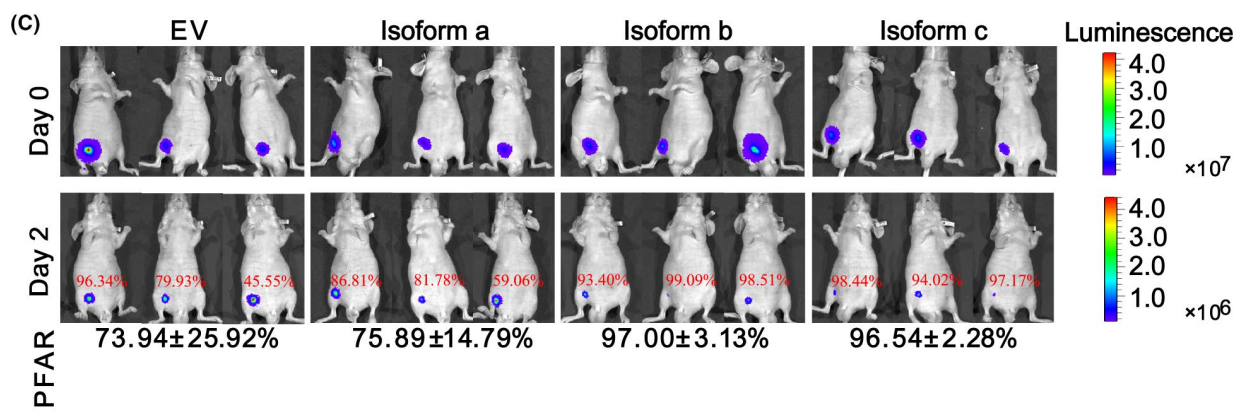
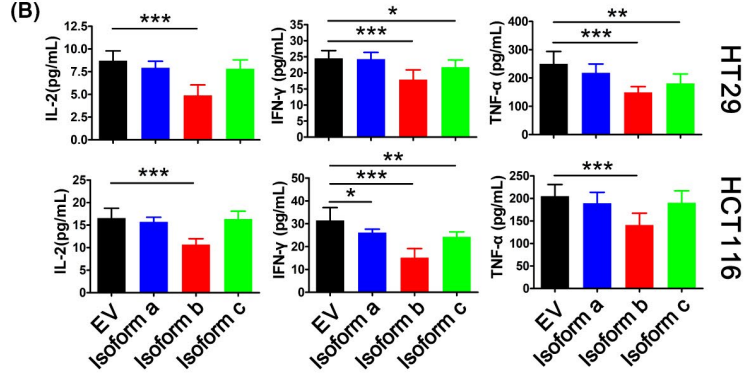
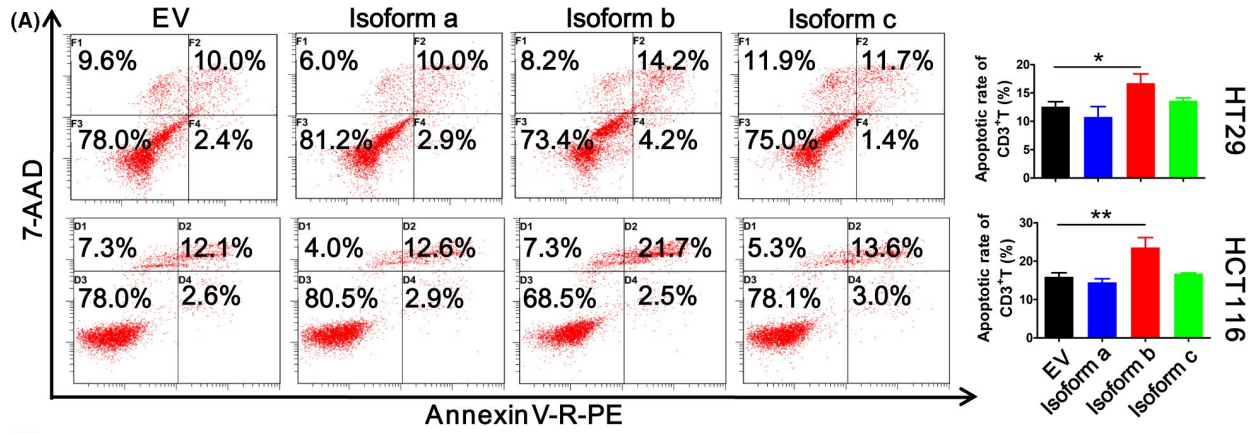


FIGURE 4 Immune regulation effects of different programmed death ligand 1 (PD-L1) isoforms on T cells in vitro and in vivo. A, Flow cytometry analysis of apoptosis of T cells which were cocultured with PD-L1 isoform-overexpressing HT29 and HCT116 cells (the histograms on the right are for the quantification analysis). B, ELISA for the detection of cytokines, including IL-2, IFN- γ , and TNF- α , in the supernatant of cocultures of T cells and PD-L1 isoform-overexpressing HT29 and HCT116 cells. C, In vivo photon flux attenuation ratio of T cells which were mixed with PD-L1 isoform-overexpressing HCT116 cells. D, Immunoblotting to detect the immunoprecipitation of exogenous FLAG-tagged PD-L1 isoforms and HA-tagged programmed death-1 (PD-1) by an anti-FLAG antibody in HEK293 cells. E, Immunoblotting to detect the immunoprecipitation of exogenous FLAG-tagged PD-L1 isoforms and HA-tagged PD-1 by an anti-HA antibody in HEK293 cells. Data are representative of three independent experiments and (A, B) were analyzed using an unpaired *t* test. Data are presented as mean \pm SD; **P* < 0.05, ***P* < 0.01, and ****P* < 0.001. PFAR, photon flux attenuation rate

isoform (Figure 5D and Figure S2D). It could be interpreted that the exogenous PD-L1 isoform vector was different from the promoter of endogenous PD-L1; many studies have shown that IFN- γ upregulates the expression of PD-L1 by affecting the transcription directly or indirectly.²⁷⁻²⁹ The IFN- γ cannot affect the expression of PD-L1 isoforms because of our experimental design. The underlying mechanism of regulation of PD-L1 isoforms by cytokines still needs to be clarified in future.

3.5 | Expression of programmed death ligand 1 and the programmed death ligand 1 isoforms in clinical colorectal cancer cell samples

Finally, we detected PD-L1 levels in two cohorts of CRC tissue samples and a cohort of serum samples by using immunohistochemistry (IHC), ELISA and qRT-PCR. According to the IHC assays, among 268 samples, there were 89 samples with PD-L1 staining positivity. Although the PD-L1 staining was focally positive in the CRC samples, the patients with positive PD-L1 expression were associated with poorer overall survival than those with negative expression (Figure 6A and Figure S4A). PD-L1 has been reported to contain a secretory signal that can be secreted into the extracellular space.^{30,31} To validate this, we ultra-filtrated and concentrated the culture medium from PD-L1 isoforms overexpressing HCT116 cells along with cell lysates for detecting PD-L1 by immunoblotting analysis. As shown in Figure 6B, the secreted PD-L1 was present in culture medium only from isoform c overexpressed HCT116 cells but not from the other two isoforms overexpressed HCT116 cells. Therefore, serum PD-L1 represents PD-L1 isoform c mainly. Then, we detected serum PD-L1 levels in 153 CRC patients and 153 healthy control donors by ELISA. The CRC group showed significantly higher serum levels of PD-L1 than the healthy control group (Figure 6C). Compared with the control group, the group of patients with high serum PD-L1 levels displayed a poorer prognosis (Figure 6D). Although isoform c is considered a secreted form of PD-L1,^{32,33} the clinical significance of the expression of the different PD-L1 isoforms in CRC remains unclear. Therefore, we designed three pairs of specific primers, one pair for each isoform of PD-L1, and detected the mRNA levels of the isoforms in 139 fresh CRC tissue samples by qRT-PCR. Among the three PD-L1 isoforms, isoform a had the highest level in CRC, and isoform b had the lowest (Figure 6E). Intriguingly, the levels of PD-L1 isoforms b and c were negatively associated with prognosis (Figure 6F). In addition, PD-L1 isoform a was not associated with

prognosis. Unexpectedly, the total PD-L1 only showed a trend that was negatively associated with prognosis, but no statistical differences were observed (Figure 6F). To further confirm the relationship between isoforms b and c and prognosis, we performed Kaplan-Meier analysis for a combination of isoforms b and c in clinical CRC samples, which showed that those with high PD-L1 isoform b and c levels had the poorest prognosis in all groups (Figure S4B). The reason for excluding PD-L1 isoform a in this combination analysis is that PD-L1 isoform a was not associated with prognosis. In summary, high PD-L1 isoform b and c levels were associated with a poor prognosis.

To investigate whether the CRC patients with high levels of PD-L1 isoform b respond well to anti-PD-1 therapy, we determined the expression of the three PD-L1 isoforms in the tumor tissues of two microsatellite stable (MSS) CRC patients without any treatment, who suffered postoperative metastatic recurrence and underwent treatment with PD-1 blockade therapy. As expected, the patient with a higher level of PD-L1 isoform b had a good response to anti-PD-1 therapy, and the lung metastases lesions were confined and liver metastasis did not occur. However, another patient with a lower level of PD-L1 isoform b did not respond to anti-PD-1 therapy and died after 2 months of PD-1 blockade treatment, with rapid deterioration due to liver metastasis and a new lung metastasis foci formation (Figure 6G). These preliminary clinical data demonstrated that PD-L1 isoform b might be an authentic biomarker of clinical response to anti-PD-1 therapy.

4 | DISCUSSION

The present study redefined the biological functions of the three PD-L1 isoforms in CRC. Among the three alternative splicing isoforms, besides being an immune checkpoint molecule, PD-L1 isoform a also played a critical role in colorectal cancer stem cell (CSC) expansion.³⁴ PD-L1 isoform b was determined to be a more effective immune checkpoint molecule that helps tumor cells escape immune surveillance. PD-L1 isoform c could be considered a prometastatic gene that promotes CRC progression; meanwhile it could be secreted to inhibit T cell activity through binding to PD-1. The existence of endogenous isoform c had been confirmed in previous studies;^{32,33} these studies also validated that endogenous isoform c could be secreted and negatively regulated T-cell function. Our clinical data demonstrated that high levels of PD-L1 isoform b and isoform c in CRC tissue

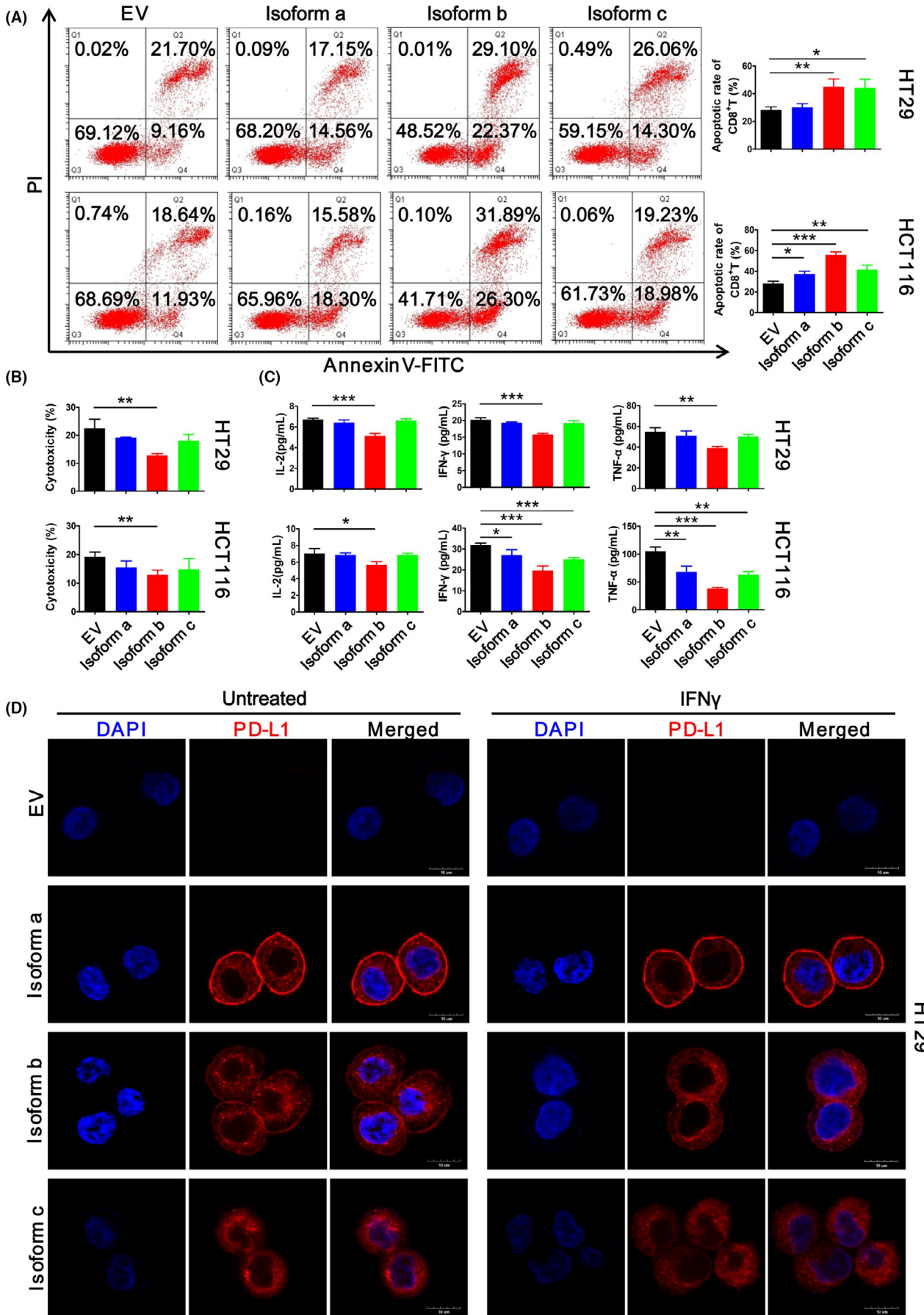


FIGURE 5 Immune regulation effects of different programmed death ligand 1 (PD-L1) isoforms on CD8⁺ T cells in vitro. A, Flow cytometry analysis of apoptosis of CD8⁺ T cells which were cocultured with PD-L1 isoform-overexpressing HT29 and HCT116 cells (the histograms on the right are for the quantification analysis). B, Cytotoxicity assays by using a cytotoxicity lactate dehydrogenase (LDH) detection kit, in the supernatant of cocultures of CD8⁺ T cells and PD-L1 isoform-overexpressing HT29 and HCT116 cells. C, ELISA for the detection of cytokines, including IL-2, IFN- γ , and TNF- α , in the supernatant of cocultures of CD8⁺ T cells and PD-L1 isoform-overexpressing HT29 and HCT116 cells. D, Immunofluorescence assay assessing the subcellular localization of the PD-L1 isoforms in HT29 cells. Data are representative of three independent experiments and (A, B, and C) were analyzed using an unpaired t test. Data are presented as mean \pm SD; * P < 0.05, ** P < 0.01, and *** P < 0.001. PD-1, programmed death 1

samples were associated with a poorer prognosis. The overexpression of PD-L1 isoform b could facilitate tumor cells escaping immune surveillance through promoting T-cell apoptosis, inhibiting T-cell proliferation, and decreasing cytokine secretion, which further enhanced tumor progression and resulted in a poor prognosis. Although PD-L1 isoform c could be secreted to inhibit T cell activity, its inhibitory effect on T cells was weaker than that of PD-L1 isoform b because of its cytoplasm location. Interestingly, PD-L1 isoform c significantly enhanced CRC proliferation, migration, and invasion through regulating EMT and also caused an unfavorable outcome. More interestingly, the serum PD-L1 level was negatively correlated with the prognosis of CRC patients, which also partly supported PD-L1 isoform c as a prometastatic gene, because only PD-L1 isoform c could be secreted from cells. In addition, PD-L1 isoform a has been reported to promote colorectal CSC expansion, which, in turn, enhances the chemoresistance and tumorigenesis of CRC cells.³⁴ Our current data provide a novel insight and a new perspective for exploring the roles of PD-L1 in immunotherapy and CRC progression. Zhou et al³⁰ identified four splice variants in addition to full-length PD-L1 in melanoma cell lines by PCR sequencing; all of these splice variants lacking the transmembrane domain could be secreted. They found that secreted PD-L1 variants exhibited inhibitory functions on T-cell activation and proliferation, and the circulating secreted PD-L1 variants were considered as prognostic biomarkers that may predict outcomes for subgroups of patients receiving checkpoint inhibitors. Gong et al³¹ identified five PD-L1 splicing variants by RNA-seq analysis in non-small cell lung cancer patients who had relapsed from PD-L1 blockade therapy, all five PD-L1 variants maintained the binding domain to PD-1 (IgV) and four of them lacked the transmembrane domain. They found that the presence of secreted PD-L1 splicing variants or the level of soluble PD-L1 in plasma or pleural effusion might work as a biomarker to predict patients' response to PD-L1 blockade therapy, and the secreted PD-L1 variants could also mediate the resistance to anti-PD-1 antibody treatment. The nucleotide and amino acid sequences for all the above reported PD-L1 isoforms were different from any PD-L1 isoforms in the present study.

To date, immune checkpoint inhibitors targeting the PD-L1/PD-1 axis have produced clinical benefits in melanoma and non-small cell lung cancer. However, some clinical trials have shown that the response rate of anti-PD-1 antibodies in CRC patients is very limited.³⁵ Even in CRC patients with PD-L1 positivity by IHC, the response rate is minimal.³⁶ The present study interpreted this

discrepancy. We found that PD-L1 isoform b had a more significant inhibitory effect on T cells than isoform a and isoform c but was expressed less in CRC. Meanwhile, we also found that in vivo experiments the inhibitory effect of isoform c on T cells is equivalent to isoform b, which may be due to the fact that isoform c can be secreted and binds to PD1. In addition, it can promote tumor cells proliferation. These results demonstrated that the development of CRC might not be primarily due to immune evasion and inhibition of the immune system but due to other molecular mechanisms. Therefore, PD1/PD-L1 checkpoint blockade would not be able to inhibit CRC progression, even if it activated the immune system.

Interestingly, several clinical trials presented unexpected results. For example, the anti-PD-1 antibody Opdivo did not show a more favorable therapeutic effect in the patients with expression of PD-L1. Even the median survival time of patients with PD-L1 expression of less than 1% was 6 months longer than those of patients with PD-L1 expression of more than 1%.³⁷ Some patients with PD-L1 negativity could also benefit from anti-PD-1 therapy, while some patients with PD-L1 positivity might not benefit.³⁸ In addition, some studies report that PD-1/PD-L1 blockade benefits patients with microsatellite instability (MSI) CRC.¹⁶ However, our data showed no significant correlation between PD-L1 expression and MSI in CRC (data not shown). Transcriptomic expression profile analysis across The Cancer Genome Atlas showed the strongest association of PD-L1 isoform c with full-length PD-L1;³³ therefore, PD-L1 positivity also means PD-L1 isoform c positivity to some extent. Thus, these findings partly support our conclusion. The antibody targeting PD-1 inhibits the apoptosis and inactivation of T cells to ensure the normal function of the immune system, but the immune system might not inhibit cancer progression ultimately because the high expression of PD-L1 isoform c can promote tumor cell proliferation, invasion, and metastasis. In this case, the patients could not get benefit from the PD-1 blockade therapy but suffer side effect.

However, only the full-length PD-L1 (PD-L1 isoform a) has been detected as a biomarker of clinical responsiveness to anti-PD-1 therapy.³⁹⁻⁴¹ Therefore, our data suggest that PD-L1 isoform b should also be considered as a biomarker for immune checkpoint blockade therapy. In addition to the fact that PD-L1 isoform b causes immune resistance, leading to poor survival in CRC patients, PD-L1 isoform c is a predictor of poor prognosis because it can not only promote CRC metastasis but can also be secreted to inhibit T cell activity. Thus, our data indicate that blocking PD-L1 involves not only regulating the immune checkpoint but also inhibiting tumor metastasis. Therefore, the PD-L1 alternative splicing isoforms should be redefined for immune checkpoint blockade

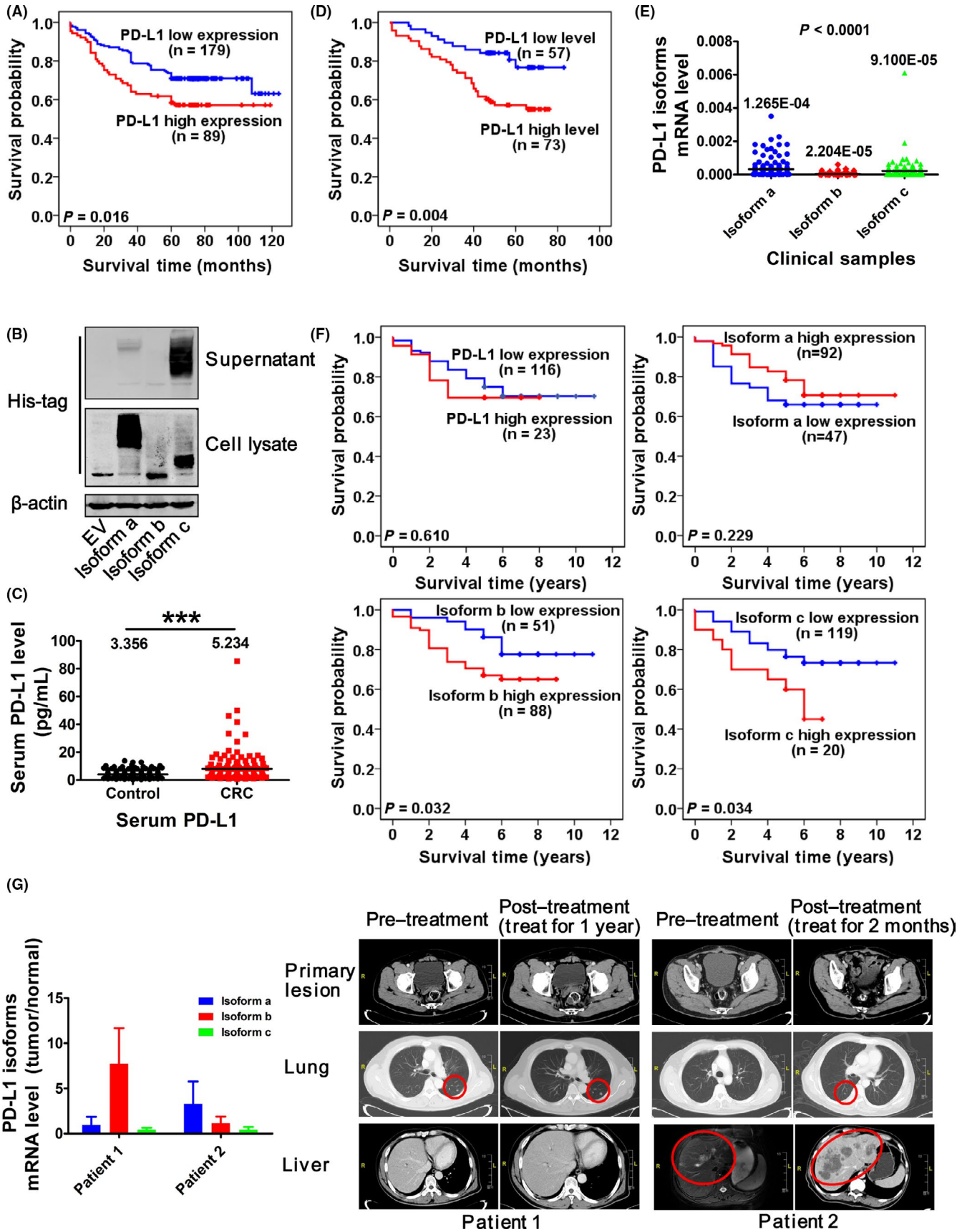


FIGURE 6 Expression of programmed death ligand 1 (PD-L1) and the PD-L1 isoforms in clinical CRC samples. A, Kaplan-Meier plots of CRC patients (n = 268) stratified into high (Over 1% tumor cells with PD-L1 positivity) and low PD-L1 expression groups. B, Immunoblotting analysis of PD-L1 isoform protein levels in transfected HCT116 cells. C, The serum level of PD-L1 in healthy control subjects and CRC patients. D, Kaplan-Meier plot of CRC patients (n = 130) stratified into high (PD-L1 > 4.41 pg/mL) and low (PD-L1 ≤ 4.41 pg/mL) PD-L1 serum level groups. E, quantitative RT-PCR (qRT-PCR) analysis of PD-L1 isoform mRNA levels in CRC patient clinical cDNA samples (n = 139). F, Kaplan-Meier plots of CRC samples (n = 139) divided into high (PD-L1: $2^{-\Delta Ct} \geq 0.001953$; isoform a: $2^{-\Delta Ct} \geq 0.000061$; isoform b: $2^{-\Delta Ct} \geq 0.000013$; isoform c: $2^{-\Delta Ct} \geq 0.000331$) and low (PD-L1: $2^{-\Delta Ct} < 0.001953$; isoform a: $2^{-\Delta Ct} < 0.000061$; isoform b: $2^{-\Delta Ct} < 0.000013$; isoform c: $2^{-\Delta Ct} < 0.000331$) PD-L1, PD-L1 isoform a, PD-L1 isoform b, and PD-L1 isoform c expression groups. G, qRT-PCR analysis of PD-L1 isoform mRNA levels in CRC patient tumor tissues samples and representative computed tomographic images of these two patients. Data (B) are representative of three independent experiments and (C) were analyzed using an unpaired t test and (E) were analyzed using a Kruskal-Wallis test. Data (C and E) are presented as medians; *P < 0.05, **P < 0.01, and ***P < 0.001. CRC, colorectal cancer; PD-L1, programmed death ligand 1

therapy because of the heterogeneous and dynamic expression of PD-L1 in tumors.

In conclusion, we highlighted the functional importance of PD-L1 isoforms b and c in mediating CRC immune evasion and progression. We also provided strong preclinical evidence for PD-L1 isoforms as potential prognostic biomarkers and/or effective targets for CRC therapy. Further investigation is necessary to clarify molecular mechanisms and to replicate our findings. Additional studies in other cancer types may be conducted to test our findings, which may be broadly applied as a novel therapeutic strategy for cancer.

ACKNOWLEDGMENTS

This work is supported by grants from the National Natural Science Foundation of China (grant numbers: 81672730, 81871937, 82072629, and 91859204), the Fundamental Research Funds for the Central Universities, and the 111 Project (B13026). We thank Mrs Q. Huang (Core Facilities, Zhejiang University School of Medicine) for the IHC technical support.

DISCLOSURE

The authors declare no conflict of interest.

DATA AVAILABILITY STATEMENT

The accession numbers for RNA-seq data are available through SRA BioProject PRJNA528362. All relevant data are available from the authors upon reasonable request.

ORCID

Chaoyan Wang  <https://orcid.org/0000-0002-2513-9178>

REFERENCES

- Wang X, Teng F, Kong L, Yu J. PD-L1 expression in human cancers and its association with clinical outcomes. *OncoTargets Therapy*. 2016;9:5023-5039.
- Lynch D, Murphy A. The emerging role of immunotherapy in colorectal cancer. *Ann Transl Med*. 2016;4:305.
- Keir ME, Butte MJ, Freeman GJ, Sharpe AH. PD-1 and its ligands in tolerance and immunity. *Annu Rev Immunol*. 2008;26:677-704.
- Butte MJ, Keir ME, Phamduy TB, Sharpe AH, Freeman GJ. Programmed death-1 ligand 1 interacts specifically with the B7-1 costimulatory molecule to inhibit T cell responses. *Immunity*. 2007;27:111-122.
- Shin T, Kennedy G, Gorski K, et al. Cooperative B7-1/2 (CD80/CD86) and B7-DC costimulation of CD4+ T cells independent of the PD-1 receptor. *J Exp Med*. 2003;198:31-38.
- Chen K, Cheng G, Zhang F, et al. Prognostic significance of programmed death-1 and programmed death-ligand 1 expression in patients with esophageal squamous cell carcinoma. *Oncotarget*. 2016;7:30772-30780.
- Geng Y, Wang H, Lu C, et al. Expression of costimulatory molecules B7-H1, B7-H4 and Foxp3+ Tregs in gastric cancer and its clinical significance. *Int J Clin Oncol*. 2015;20:273-281.
- Thompson RH, Kuntz SM, Leibovich BC, et al. Tumor B7-H1 is associated with poor prognosis in renal cell carcinoma patients with long-term follow-up. *Can Res*. 2006;66:3381-3385.
- Mittendorf EA, Philips AV, Meric-Bernstam F, et al. PD-L1 expression in triple-negative breast cancer. *Cancer Immunol Res*. 2014;2:361-370.
- Bigelow E, Bever KM, Xu H, et al. Immunohistochemical staining of B7-H1 (PD-L1) on paraffin-embedded slides of pancreatic adenocarcinoma tissue. *J Vis Exp*. 2013;(71):e4059.
- Zhou ZJ, Zhan P, Song Y. PD-L1 over-expression and survival in patients with non-small cell lung cancer: a meta-analysis. *Transl Lung Cancer Res*. 2015;4:203-208.
- Pardoll DM. The blockade of immune checkpoints in cancer immunotherapy. *Nat Rev Cancer*. 2012;12:252-264.
- Fulchiero E, Jimeno A. Nivolumab. *Drugs Today (Barcelona, Spain: 1998)*. 2014;50:791-802.
- Luke JJ, Ott PA. PD-1 pathway inhibitors: the next generation of immunotherapy for advanced melanoma. *Oncotarget*. 2015;6:3479-3492.
- Sharma P, Allison JP. Immune checkpoint targeting in cancer therapy: toward combination strategies with curative potential. *Cell*. 2015;161:205-214.
- Le DT, Uram JN, Wang H, et al. PD-1 blockade in tumors with mismatch-repair deficiency. *New Engl J Med*. 2015;372:2509-2520.
- Mezzadra R, Sun C, Jae LT, et al. Identification of CMTM6 and CMTM4 as PD-L1 protein regulators. *Nature*. 2017;549:106-110.
- Singh G, Pratt G, Yeo GW, Moore MJ. The clothes make the mRNA: past and present trends in mRNA fashion. *Annu Rev Biochem*. 2015;84:325-354.
- Calabretta S, Richard S. Emerging roles of disordered sequences in RNA-binding proteins. *Trends Biochem Sci*. 2015;40:662-672.
- He XH, Xu LH, Liu Y. Identification of a novel splice variant of human PD-L1 mRNA encoding an isoform-lacking IgV-like domain. *Acta Pharmacol Sin*. 2005;26:462-468.
- Shintani Y, Fukumoto Y, Chaika N, Svoboda R, Wheelock MJ, Johnson KR. Collagen I-mediated up-regulation of N-cadherin requires cooperative signals from integrins and discoidin domain receptor 1. *J Cell Biol*. 2008;180:1277-1289.
- Bates RC, Mercurio AM. The epithelial-mesenchymal transition (EMT) and colorectal cancer progression. *Cancer Biol Ther*. 2005;4:365-370.

23. Freeman GJ, Long AJ, Iwai Y, et al. Engagement of the Pd-1 immunoinhibitory receptor by a novel B7 family member leads to negative regulation of lymphocyte activation. *J Exp Med*. 2000;192:1027-1034.
24. Hamid O, Robert C, Daud A, et al. Safety and tumor responses with lambrolizumab (anti-PD-1) in melanoma. *New Engl J Med*. 2013;369:134-144.
25. Francisco LM, Salinas VH, Brown KE, et al. PD-L1 regulates the development, maintenance, and function of induced regulatory T cells. *J Exp Med*. 2009;206:3015-3029.
26. Parsa AT, Waldron JS, Panner A, et al. Loss of tumor suppressor PTEN function increases B7-H1 expression and immunoresistance in glioma. *Nat Med*. 2007;13:84-88.
27. Garcia-Diaz A, Shin DS, Moreno BH, et al. Interferon receptor signaling pathways regulating PD-L1 and PD-L2 expression. *Cell Rep*. 2017;19:1189-1201.
28. Cerezo M, Guemiri R, Druillennec S, et al. Translational control of tumor immune escape via the eIF4F-STAT1-PD-L1 axis in melanoma. *Nat Med*. 2018;24:1877-1886.
29. Dorand RD, Nthale J, Myers JT, et al. Cdk5 disruption attenuates tumor PD-L1 expression and promotes antitumor immunity. *Science (New York, NY)*. 2016;353:399-403.
30. Zhou J, Mahoney KM, Giobbie-Hurder A, et al. Soluble PD-L1 as a biomarker in malignant melanoma treated with checkpoint blockade. *Cancer Immunol Res*. 2017;5:480-492.
31. Gong B, Kiyotani K, Sakata S, et al. Secreted PD-L1 variants mediate resistance to PD-L1 blockade therapy in non-small cell lung cancer. *J Exp Med*. 2019;216:982-1000.
32. Hassounah NB, Malladi VS, Huang Y, et al. Identification and characterization of an alternative cancer-derived PD-L1 splice variant. *Cancer Immunol Immunother: CII*. 2019;68:407-420.
33. Mahoney KM, Shukla SA, Patsoukis N, et al. A secreted PD-L1 splice variant that covalently dimerizes and mediates immunosuppression. *Cancer Immunol Immunother: CII*. 2019;68:421-432.
34. Wei F, Zhang T, Deng SC, et al. PD-L1 promotes colorectal cancer stem cell expansion by activating HMGA1-dependent signaling pathways. *Cancer Lett*. 2019;450:1-13.
35. Toh JWT, de Souza P, Lim SH, et al. The potential value of immunotherapy in colorectal cancers: review of the evidence for programmed death-1 inhibitor therapy. *Clin Colorectal Cancer*. 2016;15:285-291.
36. O'Neil BH, Wallmark J, Lorente D, et al. 502 Pembrolizumab (MK-3475) for patients (pts) with advanced colorectal carcinoma (CRC): preliminary results from KEYNOTE-028. *Eur J Cancer*. 2015;51: S103.
37. Motzer RJ, Escudier B, McDermott DF, et al. Nivolumab versus everolimus in advanced renal-cell carcinoma. *New Engl J Med*. 2015;373:1803-1813.
38. Fusi A, Festino L, Botti G, et al. PD-L1 expression as a potential predictive biomarker. *Lancet Oncol*. 2015;16:1285-1287.
39. Reck M, Rodriguez-Abreu D, Robinson AG, et al. Pembrolizumab versus chemotherapy for PD-L1-positive non-small-cell lung cancer. *New Engl J Med*. 2016;375:1823-1833.
40. Patel SP, Kurzrock R. PD-L1 expression as a predictive biomarker in cancer immunotherapy. *Mol Cancer Ther*. 2015;14:847-856.
41. Tumei PC, Harview CL, Yearley JH, et al. PD-1 blockade induces responses by inhibiting adaptive immune resistance. *Nature*. 2014;515:568-571.

SUPPORTING INFORMATION

Additional supporting information may be found online in the Supporting Information section.

How to cite this article: Wang C, Weng M, Xia S, et al. Distinct roles of programmed death ligand 1 alternative splicing isoforms in colorectal cancer. *Cancer Sci*. 2021;112: 178-193. <https://doi.org/10.1111/cas.14690>